



# Sodium persulfate promoted interzeolite transformation of USY into SSZ-13 via a solid-state grinding route and its enhanced catalytic lifetime in the methanol-to-olefins reaction

Xinhong Zhao<sup>1</sup> · Li Niu<sup>1</sup> · Zongyi Hao<sup>1</sup> · Xuefeng Long<sup>1</sup> · Dongliang Wang<sup>1</sup> · Guixian Li<sup>1</sup>

Received: 17 September 2021 / Accepted: 27 October 2021 / Published online: 1 November 2021  
© Akadémiai Kiadó, Budapest, Hungary 2021

## Abstract

SSZ-13 has been widely used in catalysis and adsorption due to its excellent hydrothermal stability and large specific surface area. It was reported that the long crystallization time was one of the primary challenges limiting its industrial progress. In this paper, we reported a novel solid-state grinding route of synthesizing SSZ-13 zeolite, which was based on interzeolite transformation strategy and promoted by sodium persulfate ( $\text{Na}_2\text{S}_2\text{O}_8$ ). The effects of the amount of  $\text{Na}_2\text{S}_2\text{O}_8$  and crystallization time on the purity and crystallinity of SSZ-13 zeolite were studied by XRD measurements in detail. The results indicated that the crystallization time could be significantly shortened from 72 to 24 h when the molar ratio of  $\text{Na}_2\text{S}_2\text{O}_8/\text{SiO}_2$  was changed from 0 to 0.01, proving that  $\text{Na}_2\text{S}_2\text{O}_8$  has the ability of accelerating the crystallization of SSZ-13 as a hydroxyl radical reagent. Three typical SSZ-13 materials and a reference sample were used as the catalysts for methanol-to-olefins reaction (MTO) and their physicochemical properties were analyzed by SEM,  $\text{N}_2$  physisorption and  $\text{NH}_3$ -TPD techniques. The SEM characterization results showed that the crystal size of SSZ-13 synthesized in the presence of  $\text{Na}_2\text{S}_2\text{O}_8$  was larger than that of the one in the absence of it. The  $\text{NH}_3$ -TPD results showed that the introduction of  $\text{Na}_2\text{S}_2\text{O}_8$  could modulate the acid properties of SSZ-13 zeolites. The MTO tests revealed that the catalytic lifetime of one sample with  $\text{Na}_2\text{S}_2\text{O}_8$  promoter (SSZ-13-0.01M-24h) was much longer than that of the other three samples. The observed difference in catalytic stability was mainly attributed to their various concentrations of medium strong acid sites.

**Keywords** SSZ-13 zeolite · Interzeolite transformation · Sodium persulfate · Solid-phase grinding method · Methanol-to-olefins reaction

---

✉ Xinhong Zhao  
liczhaoxh@lut.edu.cn

Extended author information available on the last page of the article

## Introduction

Zeolite materials are widely used in adsorption, separation, ion exchange and catalytic reactions due to their special pore structure, high specific surface area and suitable acidity [1–4]. SSZ-13 is a kind of aluminosilicate zeolite with CHA topological structure and has two composite components of double six-membered ring and *cha* cage, which are interwoven and combined into a three-dimensional network structure. SSZ-13 has a single pore, which size is of up to 0.37 nm, belonging to the zeolite pores [5, 6]. It is now widely used in the fields of  $\text{NH}_3$ -SCR,  $\text{NO}_x$  removal in exhaust gas treatment,  $\text{CO}_2$  adsorption and separation, due to the characteristics of good hydrothermal stability, high activity, and excellent selectivity [7–14]. However, the traditional hydrothermal routes used to prepare SSZ-13 have many shortcomings such as long synthesis cycle and the use of high dosage of expensive template, which inevitably brings about a series of problems such as high synthesis costs and potential environmental pollution from wastewater and the template removal by high temperature calcination, contrary to the concept of contemporary green synthesis [15–17].

Recently, several new routes of synthesizing SSZ-13 zeolite were developed. Wang et al. [18] and Pashkova et al. [19] individually reported the solvent-free synthesis of SSZ-13 using different template and amorphous silica/aluminum sources as starting materials, which were homogenized in a mortar or a planetary mill. This route significantly reduced the amount of wastewater and improved the zeolite yield. However, the synthesis time of at least 3 days was still required. Subsequently, Xiong et al. reported the rapid interzeolite transformation of Y into SSZ-13 in the presence of crystal seeds [6]. The synthesis time can be shortened to 1 day. However, the molar ratio of SDA/ $\text{SiO}_2$  is up to 0.14 in these syntheses [structure-directing agent (SDA)]. Miyagawa et al. successfully prepared SSZ-13 zeolite via the interzeolite transformation route under solvent/SDA-free conditions. This process can be completed within 18 h [20]. However, the resultant product was accompanied by PHI-type zeolite impurity.

In recent years, Yu's group discovered that hydroxyl radicals existed in the hydrothermal synthesis system of zeolite and could significantly accelerate the crystallization of zeolite [21]. Sun's group reported for the first time that the introduction of hydroxyl radicals ( $\cdot\text{OH}$ ) can promote the isomorphous substitution of silicon for germanium under mild conditions, resulting in titanosilicates zeolite with high hydrothermal stability [22]. Cheng et al. reported that in the  $\text{SiO}_2$ -TPAOH- $\text{H}_2\text{O}$  hydrothermal reaction system, sodium persulfate ( $\text{Na}_2\text{S}_2\text{O}_8$ ) can be used as an efficient additive to accelerate the synthesis of zeolite. In the presence of 0.02 M  $\text{Na}_2\text{S}_2\text{O}_8$ , the time for hydrothermal synthesis of Silicalite-1 zeolite with high crystallinity was shortened from 24 to 16 h [23]. This method provides an effective green route for the synthesis of zeolite. Zhao's group reported that FeAPO-5 [24] and Fe-ZSM-5 [25] with high crystallinity were synthesized in much shorter crystallization time by adding Fenton reagent in a solvent-free system.

Inspired by above intriguing findings, here a solid-state grinding route based on interzeolite transformation was employed to prepare SSZ-13 zeolite in this

study, in which  $\text{Na}_2\text{S}_2\text{O}_8$  was introduced to the precursor gels, aiming at accelerating the crystallization process and reducing the synthesis cost. The influences of the amount of  $\text{Na}_2\text{S}_2\text{O}_8$  and crystallization time on the synthesis of SSZ-13 were explored. The characteristic samples were selected and their catalytic lifetime was evaluated with MTO reaction as a probe.

## Experimental procedure

### Materials

All chemicals and reagents were used as received without further purification. Sodium hydroxide (96%, Sinopharm Chemical Reagent Co. Ltd.), potassium hydroxide (96%, Sinopharm Chemical Reagent Co. Ltd.), fumed silica (Aladdin), *N,N,N*-trimethyl-1-adamantammonium hydroxide (TMAdaOH, 25% in water, Hubei Jusheng Technology Co. Ltd.), USY zeolite (Si/Al = 11.5, The Catalyst Plant of Nankai University), sodium persulfate (98%, Shanghai Guangnuo Chemical Reagent Co. Ltd.) and deionized water.

### Synthesis

#### Conversion of USY zeolite to SSZ-13 with $\text{Na}_2\text{S}_2\text{O}_8$

SSZ-13 zeolites were synthesized by a solid-state grinding route with the gel molar ratio of  $\text{Na}_2\text{O}$ :  $\text{Al}_2\text{O}_3$ :  $\text{SiO}_2$ : TMAdaOH:  $\text{H}_2\text{O}$ :  $\text{Na}_2\text{S}_2\text{O}_8$  = 0.05: 0.05: 1: 0.08: 2.8:  $x$  ( $x=0, 0.005, 0.01, 0.02, 0.05$ ). In a typical run, 0.99 g of USY zeolite, 0.01 g of  $\text{Na}_2\text{S}_2\text{O}_8$  and 0.625 g of fumed silica were placed in a mortar. Then, 0.2 g of NaOH was dissolved in 1.759 g of TMAdaOH aqueous solution and added into the mortar. The mixture was homogenized by pestle for 10–20 min and then transferred into sealed stainless-steel autoclaves equipped with modified Teflon liners, which was heated at 160 °C for 24–72 h. After the crystallization process has finished, the product was recovered by filtration, washed completely with deionized water, and dried in oven at 110 °C. The product was then calcined in air at 550 °C for 6 h. After calcination, the samples were ion-exchanged with 1 M solution of  $\text{NH}_4\text{NO}_3$  at 80 °C for 3 h and then calcined in air at 550 °C for 4 h. The entire ion-exchange and further calcination procedure was repeated for three times to obtain H-form SSZ-13, which were used in MTO reaction. The resultant products were designated as SSZ-13-X-Y (X: the molar ratio of  $\text{Na}_2\text{S}_2\text{O}_8/\text{SiO}_2$  (i.e. 0, 0.005, 0.01, 0.02, 0.05 mol; Y: crystallization time, i.e. 24, 48, 72 h). According to the reference [19] a SSZ-13 reference sample was prepared under solvent-free conditions using amorphous silica and aluminum sources as the starting materials, and denoted as SSZ-13-RS.

### Characterization methods

The phase purity and crystallinity of the samples were analyzed by a D/Max-2400 Rigaku diffractometer, which was operated under the conditions of 40 kV and

150 mA with Cu  $K_{\alpha}$  as the radiation source. A JSM-6701F instrument equipped with an energy dispersive spectrometer (EDS) was used to record scanning electron microscope (SEM) images to observe the morphology and crystal size of SSZ-13. After the samples had been degassed at 150 °C for 4 h on a Micromeritics 2020 analyzer, nitrogen physisorption measurements were performed at  $-196$  °C. According to IUPAC's recommendation, the Brunauer–Emmett–Teller (BET) surface area is calculated from the linear part of the BET diagram. A Micromeritics AutoChem II 2920 automatic chemical adsorption analysis device was used to perform temperature-programmed ammonia desorption ( $\text{NH}_3$ -TPD) experiments to characterize the acidity of the samples.

## MTO reaction

The menthol-to-olefins reaction was performed in a fixed-bed reactor made of a stainless quartz tube, at 400 °C and atmospheric pressure. Prior to the reaction, 30 mg of SSZ-13 catalyst was packed in the center of quartz wools and activated in a  $\text{N}_2$  flow of 30 mL/min at 500 °C for 1 h and then cooled to the reaction temperature. Methanol as the reactant was fed by passing the carrier gas ( $\text{N}_2$ , 15 mL/min) into the reactor at 400 °C, which resulted in the weight hourly space velocity (WHSV) of  $3.0 \text{ h}^{-1}$ . The effluents were detected by an online gas chromatograph GC7900 system (Tianmei, Shanghai, China) equipped with a flame ionization detector (FID) and Plot-Q column.

## Results and discussion

### XRD analysis

At first, we optimized the synthesis of SSZ-13 samples in the absence of  $\text{Na}_2\text{S}_2\text{O}_8$  and additional water, for which USY zeolite and fumed silica were used as the main raw materials. It was found that the optimum initial composition for this material was  $\text{Na}_2\text{O} : \text{Al}_2\text{O}_3 : \text{SiO}_2 : \text{TMAdaOH} : \text{H}_2\text{O} = 0.05 : 0.05 : 1 : 0.08 : 2.8$ , and the suitable crystallization time and crystallization temperature were 160 °C and 72 h, respectively. Obviously, in this case the molar ratio of  $\text{TMAdaOH}/\text{SiO}_2 = 0.08$  was lower than that of the data in the literature [6]. Low dosage of TMAdaOH means reduced synthesis cost and environmental pollution from SDA removal by calcination. It can be seen that the XRD pattern of SSZ-13-0M-72h (Fig. 1) synthesized under the optimized conditions is consistent with that of standard SSZ-13 (PDF#47-0762), indicating that USY zeolite was successfully converted into SSZ-13 zeolite. Its crystallinity is only slightly lower than that of the reference sample SSZ-13-RS. However, the crystallization time of SSZ-13-0M-72h is still longer in comparison to the reference data, as indicated in the introduction section. It should be mentioned that pure SSZ-13 sample cannot be obtained when the crystallization time was reduced to 48 h (not shown).

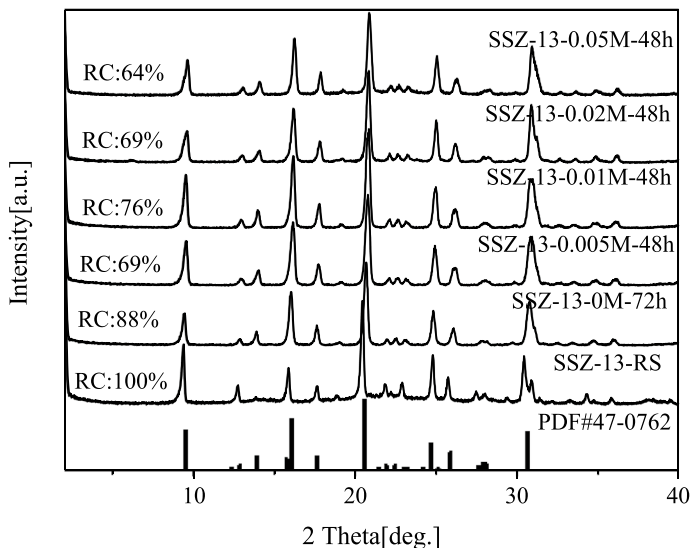


**Fig. 1** XRD patterns of five typical SSZ-13 samples synthesized under the conditions of different  $\text{Na}_2\text{S}_2\text{O}_8/\text{SiO}_2$  ratio and crystallization time, together with a reference sample. *RC* relative crystallinity

It is well known that the introduction of hydroxyl radicals ( $\bullet\text{OH}$ ) in the initial gel mixture can significantly accelerate the zeolite synthesis process, since they are more effective in the depolymerization and the polymerization of silicate gels than hydroxide ions ( $\text{OH}^-$ ) [21, 23, 26, 27]. In order to shorten the crystallization time of SSZ-13 zeolite and reduce the energy consumption, different amount of  $\text{Na}_2\text{S}_2\text{O}_8$  was introduced to the synthesis system, and the synthesis was carried out at the crystallization time of 48 h. As can be seen from Fig. 1, all products at 48 h revealed pure SSZ-13 phase, of which the sample SSZ-13-0.01M-48h exhibited the highest relative crystallinity. However, the crystallinity of these samples is lower than that of SSZ-13-0M-72h and the reference sample (SSZ-13-RS), which meant that the former perhaps contained more lattice defect or were not well crystallized. In order to further reduce the energy consumption, the synthesis time was shortened to 24 h and the XRD patterns of the resulting products are shown in Fig. 2. It can be found that only the sample SSZ-13-0.01M-24h was of pure SSZ-13 material, while other samples displayed the diffraction patterns attributed to USY zeolite. This result indicated that the USY raw material failed to be converted into the targeted SSZ-13. It should be noted that the crystallinity of SSZ-13-0.01M-24h was comparable to that of the samples synthesized at 48 h. This result proved that  $\text{Na}_2\text{S}_2\text{O}_8$  did have the function of accelerating the crystallization of SSZ-13 zeolite.

## SEM analysis

The morphology of a series of representative SSZ-13 products (SSZ-13-0M-72h, SSZ-13-0.01M-24h, SSZ-13-0.01M-48h, and SSZ-13-RS) was investigated by

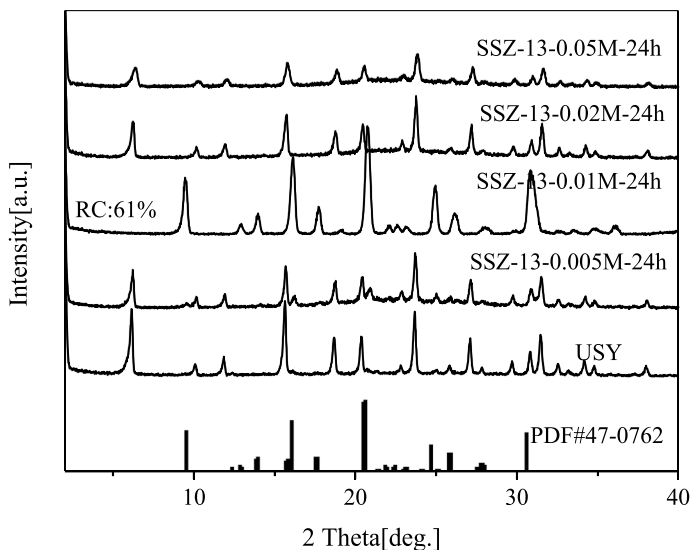


**Fig. 2** XRD patterns of four samples synthesized under the conditions of crystallization time of 24 h and different  $\text{Na}_2\text{S}_2\text{O}_8/\text{SiO}_2$  ratio, together with a USY sample as the reference. *RC* relative crystallinity

SEM, and the corresponding micrographs are shown in Fig. 3. It can be seen that the sample SSZ-13-0M-72h is composed of cubic crystals with a size of about 50–100 nm. However, evident cracks can be observed on its coarse surface (Fig. 3a, e). In contrast, the samples SSZ-13-0.01M-24h and SSZ-13-0.01M-48h appear as smooth cubic crystals with a size of 1  $\mu\text{m}$ . Nevertheless, a small amount of amorphous phase can be found to be attached to the cubic crystals. This may be explained by their shortened crystallization time. The depolymerized silica and aluminum sources failed to completely interact with the template, and reorganize and polymerize the amorphous materials to form crystalline SSZ-13. In addition, the reference sample H-SSZ-13-RS is mainly comprised of 0.4–2  $\mu\text{m}$  cubic crystals. No apparent amorphous particles can be observed, demonstrating its high relative crystallinity.

### Textural analysis

Fig. 4 displays the  $\text{N}_2$  absorption/desorption isotherms of the SSZ-13 samples and the specific textural parameters are provided in Table 1. It can be revealed that the sample SSZ-13-0M-72h shows I-type adsorption isotherm, suggesting that it is a typical microporous material. Moreover, in the high relative pressure zone ( $P/P_0 \geq 0.8$ ) of this isotherm, a distinct hysteresis loop can be discovered, indicating that this sample contains additional mesopores or macropores due to the aggregation of nanoparticles. By contrast, the adsorption isotherms of the samples SSZ-13-0.01M-48h and SSZ-13-0.01M-24h resemble that of SSZ-13-0M-72h, but exhibit unapparent hysteresis loop. This result suggests that SSZ-13-0.01M-48h and SSZ-13-0.01M-24h are microporous materials with small amount of mesopores/macropores. As a

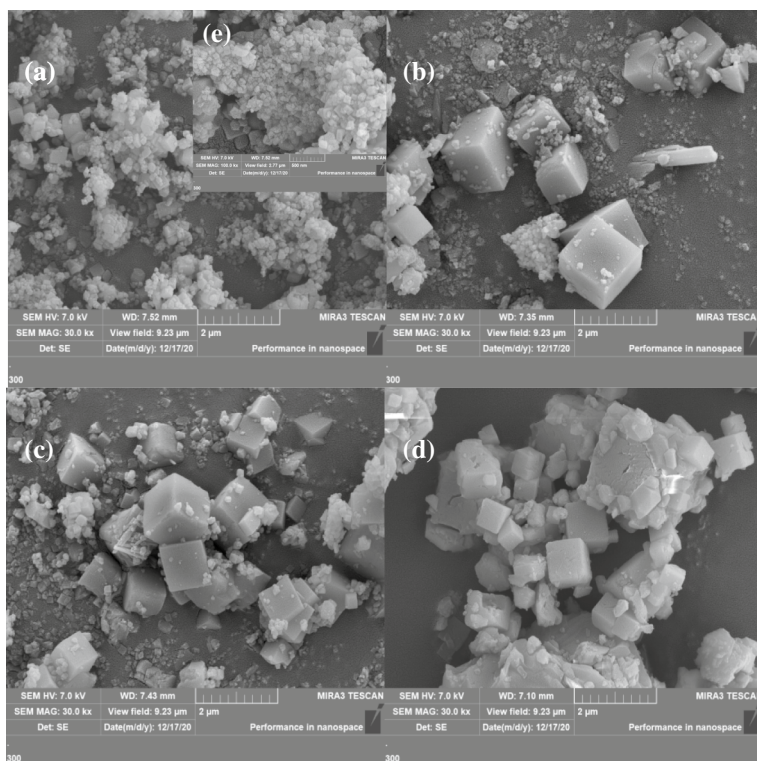


**Fig. 3** The SEM micrographs of a reference sample and three SSZ-13 samples synthesized under the conditions of different dosage of sodium persulfate and crystallization time: **a**, **e** SSZ-13-0M-72h; **b** SSZ-13-0.01M-24h; **c** SSZ-13-0.01M-48h; **d** SSZ-13-RS. Among them, **e** is the SEM micrograph of the sample SSZ-13-0M-72h at 500 nm

comparison, no evident hysteresis loop can be observed in the isotherm of the reference sample SSZ-13-RS. This means that this sample is a purely microporous material.

It can be seen from Table 1 that the sample SSZ-13-0M-72h exhibits the highest mesoporous volume among the four samples, as can be evidenced by the obvious hysteresis loop at  $P/P_0 \geq 0.8$  in the isotherm. It is worthwhile to note that the reference sample SSZ-13-RS has the largest external surface area. This result may be explained by the fact that this sample contains large amount of nano-sized discrete cubic crystals (Fig. 3). In addition, the sample SSZ-13-0.01M-24h exhibits the largest BET surface area and microporous volume although its crystallinity is not the highest for the four samples.

### Acid analysis ( $\text{NH}_3$ -TPD)

Fig. 5 shows  $\text{NH}_3$ -TPD curves of all SSZ-13 zeolites. The acid concentration parameters are listed in Table 1. It can be seen from Fig. 5 that all samples show



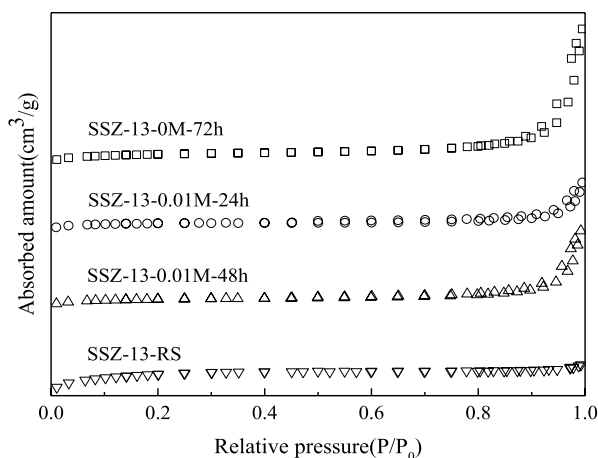


**Fig. 4**  $N_2$  adsorption/desorption isotherms of a reference sample and three SSZ-13 samples synthesized under the conditions of different dosage of sodium persulfate and crystallization time

two symmetrical desorption peaks of ammonia centered at 170 °C and 420–500 °C, which correspond to the acidic sites of different acid strength. The  $NH_3$  desorption peaks at low temperatures are relevant to weak acid sites, which are mainly attributed to silanol groups on the external surface or at lattice defects and OH groups bound to aluminum species at the extra-framework [28]. It is generally accepted that the low-alkaline methanol molecules cannot be converted to light olefins at 400 °C in the weak acidic sites [29, 30]. The desorption peak at high temperature is due to the interaction of ammonia molecules with the medium strong acid centers, i.e. the Brønsted acid centers, which will greatly affect the catalytic performance of MTO. As shown in Fig. 5 and Table 1, the acid strength order of the medium strong acid sites of these samples is  $SSZ-13-0.01M-48h > SSZ-13-0.01M-24h \approx SSZ-13-0M-72h > SSZ-13-RS$ , while for the acid density, it is  $SSZ-13-0M-72h > SSZ-13-0.01M-24h > SSZ-13-0.01M-48h \approx SSZ-13-RS$ .

### Catalytic lifetime

For MTO catalysts, the catalytic lifetime was generally considered as the key one of the multiple factors affecting their industrial application. In this study, the evolution of methanol conversion for the MTO reaction over four representative SSZ-13 samples was evaluated on a fixed bed reactor and the results are shown in Fig. 6 and Table 2. The catalytic lifetime is defined as the duration time of methanol conversion over 99%. For comparison purpose, the pore structure parameters, the crystal size, acidity parameters and catalytic lifetime data of these catalysts are summarized in Table 2.

It can be seen from Fig. 6 and Table 2 that the catalytic lifetime order is  $SSZ-13-0.01M-24h$  (210 min)  $>$   $SSZ-13-0.01M-48h$  (60 min)  $>$   $SSZ-13-RS$  (20 min)  $>$



**Table 1** Textural properties and acid amount of a reference sample and three SSZ-13 samples synthesized under the conditions of different dosage of sodium persulfate and crystallization time

Sample	Textural properties					Acid amount (mmol g <sup>-1</sup> )			Total acid
	S <sub>BET</sub> /(m <sup>2</sup> g <sup>-1</sup> )	S <sub>Ext</sub> /(m <sup>2</sup> g <sup>-1</sup> )	S <sub>Micro</sub> /(m <sup>2</sup> g <sup>-1</sup> )	V <sub>Micro</sub> <sup>a</sup> /(cm <sup>3</sup> g <sup>-1</sup> )	V <sub>Meso</sub> <sup>b</sup> /(cm <sup>3</sup> g <sup>-1</sup> )	Weak acid	Medium strong acid		
SSZ-13-RS	582	83	499	0.232	0.048	0.288	0.209	0.497	
SSZ-13-0.01M-24h	616	16	600	0.281	0.075	1.372	0.421	1.793	
SSZ-13-0.01M-48h	606	22	583	0.273	0.123	1.415	0.184	1.599	
SSZ-13-0M-72h	601	32	569	0.266	0.220	1.131	0.530	1.661	

<sup>a</sup>t<sub>r</sub>-plot micropore volume; <sup>b</sup>BJH adsorption cumulative volume of pores between 1.7 and 300 nm

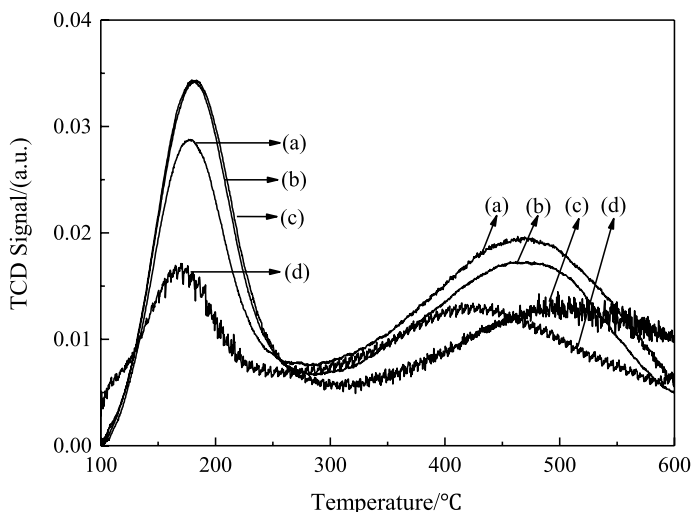


**Fig. 5**  $\text{NH}_3$ -TPD profiles of a reference sample and three SSZ-13 samples synthesized under the conditions of different dosage of sodium persulfate and crystallization time: (a) SSZ-13-0M-72h; (b) SSZ-13-0.01M-24h; (c) SSZ-13-0.01M-48h; (d) SSZ-13-RS

SSZ-13-0M-72h (10 min). It was reported that smaller crystal size (or large mesoporous volume) can enhance the mass transfer of reactants and products, thus resulting in prolonged catalytic lifetime for MTO reaction [30, 31]. However, the sample SSZ-13-0M-72h, which crystal size is the smallest, exhibits the shortest catalytic lifetime. This result implies that the acid properties of SSZ-13 catalysts may play a decisive role in determining their catalytic lifetime. As reported elsewhere, some researchers considered that medium strong acid sites have close relationship with the catalytic behavior of MTO reaction [30]. It was reasonable to speculate from Table 2 that appropriate density of medium strong acid sites may be in favor of improving the catalytic stability. For SSZ-13-RS and SSZ-13-0.01M-48h, their fast deactivation may be relevant to the coverage of the low density of medium strong acid sites by deposited carbon, while for SSZ-13-0M-72h, the presence of large amount of medium strong acid sites speeds up the coking process, thus leading to its reduced catalytic lifetime. Many researchers considered that the acidity and morphology of the MTO catalysts played the decisive roles in terms of the catalytic performance [15, 31–34]. According to our results, in order to further improve the catalytic performance of SSZ-13, its acidity and mass transfer property, especially the former, need to be precisely regulated.

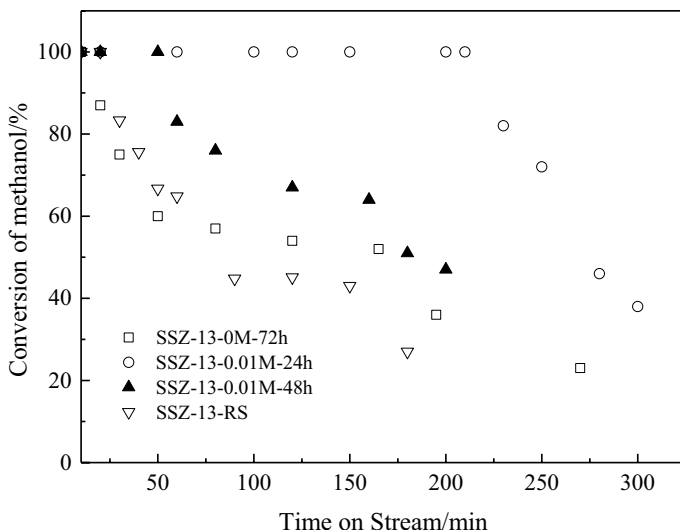


**Fig. 6** Methanol conversion over a reference sample and three SSZ-13 samples synthesized under the conditions of different dosage of sodium persulfate and crystallization time with time-on-stream in the MTO reaction

**Table 2** Summary of crystal size, medium strong acid concentration, mesoporous volume and catalytic lifetime of a reference sample and three SSZ-13 catalysts synthesized under the conditions of different dosage of sodium persulfate and crystallization time

Samples	Crystal size	Medium strong acid (mmol/g)	$V_{\text{Meso}}$ ( $\text{cm}^3 \text{g}^{-1}$ )	TOS (min)
SSZ-13-RS	0.4–2 $\mu\text{m}$	0.209	0.048	20
SSZ-13-0.01M-24h	$\leq 1 \mu\text{m}$	0.421	0.075	210
SSZ-13-0.01M-48h	$\leq 1 \mu\text{m}$	0.184	0.123	60
SSZ-13-0M-72h	50–100 nm	0.530	0.220	10

## Conclusions

In summary, USY zeolite as main starting material is successfully converted into pure SSZ-13 at a low molar ratio of TMAOH/SiO<sub>2</sub> using a solid-state grinding route. Especially, when a suitable amount of sodium persulfate promoter is introduced into the precursor gels, the crystallization time can be effectively shortened to 24 h. In addition, this sodium persulfate mediated synthesis route can reduce the density of medium strong acidic sites of SSZ-13, the catalytic active centers of MTO reaction. Among four typical SSZ-13 catalysts, SSZ-13-0.01M-24h with appropriate acid strength and concentration performed well with a catalytic lifetime of 210 min in the MTO probe reaction. The synthetic approach reported here may lead a new avenue for the inexpensive fabrication of superior-performance MTO catalysts.

**Acknowledgements** This work was supported by the National Natural Science Foundation of China (Grant Nos. 21666019, 22168022)


## References

1. Campo PD, Martínez C, Corma A (2021) Activation and conversion of alkanes in the confined space of zeolite-type materials. *Chem Soc Rev* 50:8511–8595
2. Dusselier M, Davis ME (2018) Small-pore zeolites: synthesis and catalysis. *Chem Rev* 118:5265–5329
3. Jiang N, Shang R, Heijman SGJ, Rietveld LC (2018) High-silica zeolites for adsorption of organic micro-pollutants in water treatment: a review. *Water Res* 144:145–161
4. Zhang Q, Yu J, Corma A (2020) Applications of zeolites to C1 chemistry: recent advances, challenges, and opportunities. *Adv Mater* 32(44):1–31
5. Kumar M, Luo H, Roman-Leshkov Y, Rimer JD (2015) SSZ-13 crystallization by particle attachment and deterministic pathways to crystal size control. *J Am Chem Soc* 137(40):13007–13017
6. Xiong X, Yuan D, Wu Q, Chen F, Meng X, Lv R, Dai D, Maurer S, McGuire R, Feyen M, Müller U, Zhang W, Yokoi T, Bao X, Gies H, Marler B, Vos DED, Kolb U, Moini A, Xiao F (2017) Efficient and rapid transformation of high silica CHA zeolite from FAU zeolite in the absence of water. *J Mater Chem A* 5(19):9076–9080
7. Xie K, Jungwon W, Diana B, Ashok K, Krishna K, Louise O (2018) Insights into hydrothermal aging of phosphorus-poisoned Cu–SSZ-13 for NH<sub>3</sub>–SCR. *Appl Catal B* 241:205–216
8. Proding S, Derewinski MA, Wang Y, Washton NM, Walter ED, Szanyi J, Gao F, Wang Y, Peden CHF (2017) Sub-micron Cu/SSZ-13: synthesis and application as selective catalytic reduction (SCR) catalysts. *Appl Catal B* 201:461–469
9. Hudson MR, Queen WL, Mason JA, Fickel DW, Lobo RF, Brown CM (2012) Unconventional, highly selective CO<sub>2</sub> adsorption in zeolite SSZ-13. *J Am Chem Soc* 134(4):1970–1973
10. Liang J, Su J, Wang Y, Lin Z, Mu W, Zheng H, Zou R, Liao F, Lin J (2014) CHA-type zeolites with high boron content: synthesis, structure and selective adsorption properties. *Microporous Mesoporous Mater* 194:97–105
11. Zhu X, Hofmann JP, Mezari B, Kosinov N, Wu L, Qian Q, Weckhuysen BM, Asahina S, Ruiz-Martínez J, Hensen EJM (2016) Trimodal porous hierarchical SSZ-13 zeolite with improved catalytic performance in the methanol-to-olefins reaction. *ACS Catal* 6:2163–2177
12. Luo J, Gao F, Kamasamudram K, Currier N, Peden CHF, Yezerets A (2017) New insights into Cu/SSZ-13 SCR catalyst acidity. Part I: nature of acidic sites probed by NH<sub>3</sub> titration. *J Catal* 348:291–299
13. Deimund MA, Harrison L, Lunn JD, Liu Y, Malek A, Shayib R, Davis ME (2016) Effect of heteroatom concentration in SSZ-13 on the methanol-to-olefins reaction. *ACS Catal* 6:542–550
14. Zhu X, Kosinov N, Hofmann JP, Mezari B, Qian Q, Rohling R, Weckhuysen BM, Ruiz-Martínez J, Hensen EJM (2016) Fluoride-assisted synthesis of bimodal microporous SSZ-13 zeolite. *Chem Commun* 52:3227–3230
15. Sommer L, Krivokapic A, Svelle S, Lillerud KP, Stöcker M, Olsbye U (2011) Enhanced catalyst performance of zeolite SSZ-13 in the methanol to olefin reaction after neutron irradiation. *J Phys Chem C* 115(14):6521–6530
16. Han L, Zhao X, Yu H, Hu Y, Li D, Sun D, Liu M, Chang L, Bao W, Wang J (2018) Preparation of SSZ-13 zeolites and their NH<sub>3</sub>-selective catalytic reduction activity. *Microporous Mesoporous Mater* 261:126–136
17. Wu L, Degirmenci V, Magusin PCMM, Lousberg NJHGM, Hensen EJM (2013) Mesoporous SSZ-13 zeolite prepared by a dual-template method with improved performance in the methanol-to-olefins reaction. *J Catal* 298:27–40
18. Wang X, Wu Q, Chen C, Pan S, Zhang W, Meng X, Maurer S, Feyen M, Müller U, Xiao F (2015) Atom-economical synthesis of a high silica CHA zeolite using a solvent-free route. *Chem Commun* 51(95):16920–16923
19. Pashkova V, Mlekodaj K, Klein P, Brabec L, Zouzelka R, Rathousky J, Tokarova V, Dedecek J (2019) Mechanochemical pretreatment for efficient solvent-free synthesis of SSZ-13 zeolite. *Chem—A Eur J* 25(52):12068–12073

20. Miyagawa S, Miyake K, Hirota Y, Nishiyama N, Miyamoto M, Oumi Y, Tanaka S (2019) Solvent/OSDA-free interzeolite transformation of FAU into CHA zeolite with quantitative yield. *Microporous Mesoporous Mater* 278:219–224
21. Feng G, Cheng P, Yan W, Boronat M, Li X, Su J, Wang J, Li Y, Corma A, Xu R, Yu J (2016) Accelerated crystallization of zeolites via hydroxyl free radicals. *Science* 351(6278):1188–1191
22. Shi D, Xu L, Chen P, Ma T, Lin C, Wang X, Xu D, Sun J (2019) Hydroxyl free radical route to the stable siliceous Ti-UTL with extra-large pores for oxidative desulfurization. *Chem Commun* 55(10):1390–1393
23. Cheng P, Feng G, Sun C, Xu W, Su J, Yan W, Yu J (2018) An efficient synthetic route to accelerate zeolite synthesis via radicals. *Inorg Chem Front* 5:2106–2110
24. Zhao X, Duan W, Zhang X, Ji D, Yu Z, Li G (2018) Insights into the effects of modifying factors on the solvent-free synthesis of FeAPO-5 catalysts towards phenol hydroxylation. *React Kinet Mech Catal* 125:1055–1070
25. Han Z, Zhang F, Zhao X (2019) Green energy-efficient synthesis of Fe-ZSM-5 zeolite and its application for hydroxylation of phenol. *Microporous & Mesoporous Materials* 290:109679
26. Wang J, Liu P, Boronat M, Ferri P, Xu Z, Liu P, Shen B, Wang Z, Yu J (2020) Organic-free synthesis of zeolite Y with high Si/Al ratios: combined strategy of in situ hydroxyl radical assistance and post-synthesis treatment. *Angew Chem Int Ed* 59(39):17225–17228
27. Feng G, Wang J, Boronat M, Li Y, Su J, Huang J, Ma Y, Yu J (2018) Radical-facilitated green synthesis of highly ordered mesoporous silica materials. *J Am Chem Soc* 140:4770–4773
28. Xu S, Zheng A, Wei Y, Chen J, Li J, Chu Y, Zhang M, Wang Q, Zhou Y, Wang J (2013) Direct observation of cyclic carbenium ions and their role in the catalytic cycle of the methanol-to-olefin reaction over chabazite zeolites. *Angew Chem Int Ed* 52(44):11564–11568
29. Izadbakhsh A, Farhadi F, Khorasheh F, Sahebdehfar S, Asadi M, Yan Z (2009) Effect of SAPO-34's composition on its physico-chemical properties and deactivation in MTO process. *Appl Catal A* 364(1–2):48–56
30. Bing L, Tian A, Wang F, Yi K, Sun X, Wang G (2018) Template-free synthesis of hierarchical SSZ-13 microspheres with high MTO catalytic activity. *Chem—A Eur J* 24:7428–7433
31. Xu Z, Li J, Huang Y, Ma H, Qian W, Zhang H, Ying W (2019) Size control of SSZ-13 crystals with APAM and its influence on the coking behaviour during MTO reaction. *Catal Sci Technol* 9(11):2888–2897
32. Bleken F, Bjørgen M, Palumbo L, Bordiga S, Svelle S, Lillerud KP, Olsbye U (2009) The effect of acid strength on the conversion of methanol to olefins over acidic microporous catalysts with the CHA topology. *Top Catal* 52(3):218–228
33. Zhang D, Lu H, Su N, Li G, Zhao X (2021) Property modulation of SAPO-34 with activated seeds and its enhanced lifetime in methanol to olefins reaction. *J Inorg Mater* 36(1):101–106
34. Wu L, Degirmenci V, Magusin PCMM, Szyja BM, Hensen EJM (2012) Dual template synthesis of a highly mesoporous SSZ-13 zeolite with improved stability in the methanol-to-olefins reaction. *Chem Commun* 48:9492–9494

**Publisher's Note** Springer Nature remains neutral with regard to jurisdictional claims in published maps and institutional affiliations.

## Authors and Affiliations

Xinhong Zhao<sup>1</sup>  · Li Niu<sup>1</sup> · Zongyi Hao<sup>1</sup> · Xuefeng Long<sup>1</sup> · Dongliang Wang<sup>1</sup> · Guixian Li<sup>1</sup>

<sup>1</sup> Key Laboratory of Low Carbon Energy and Chemical Engineering of Gansu Province, School of Petrochemical Technology, Lanzhou University of Technology, Lanzhou 730050, China